arXiv:cond-mat/9709089v1 8 Sep 1997

Behavior of excitonic levels in symmetric and asymmetric double quantum wells in a magnetic field

Francisco Vera and Zdenka Barticevic
Universidad Técnica Federico Santa María, casilla 110-V Valparaíso, Chile

(February 1, 2008)

We studied theoretically the excitonic energy levels and the optical absorption spectra for double quantum wells,both symmetric and asymmetric, in the presence of an homogeneous magnetic field. Within the effective mass approach, we expanded the excitonic wave-function, in an orthogonal basis formed by products of electron and hole wave-functions in the growth direction z, and one particle solutions of the magnetic Hamiltonian in the $x-y$ plane. We applied our method to the case of $Al_xGa_{1-x}As$, for which we showed how the exciton wave-function vary, and how the basis functions are mixed in a non trivial way by the effect of the Coulomb potential. By taking into account all the mixing between the elements in our base, we get anti-crossings between excited excitonic states not reported previously.

73.20.Dx,71.35.Ji

I. INTRODUCTION

In double quantum wells, excitons are more complex than in a single quantum well, because the electron and hole wave-functions can be localized either in the same well, or in different wells, or in both. The asymmetry of the quantum well produces transitions which are prohibited in the optical spectrum, of the symmetric case.

The theoretical study of excitons in double quantum wells, began with the work of Kamizato and Matsuura[1]. They studied the excitonic levels and binding energy of symmetric wells as a function of the wells and barrier widths. Dignam and Sipe[2] improved the calculation for the excitonic levels behavior for wide barriers, incorporating the Coulomb interaction between excitonic states. Their work included both symmetric and asymmetric wells, and the presence of an external electric field (see also Ref. 3), but their method of calculation is not suitable for thin barriers. Cen and Bajaj[4] improved the variational method used in Ref. 1, obtaining the exciton binding energy, in symmetric wells in an external magnetic field, for arbitrary wells and barrier width. Recently Dzyubenko and Yablonskii[5], using a non variational method, studied the excitonic levels for symmetric and almost symmetric double quantum wells, as a function of the electric and magnetic field strength. For an experimental study of excitonic levels in $Al_xGa_{1-x}As$ symmetric double quantum wells see Bayer *et al*[6], and for a recent review in the subject of excitons in double quantum wells, see Ref. 7.

In this work, we studied the excitonic levels, binding energy and optical transition probabilities, in symmetric and asymmetric double quantum wells, in the presence of a magnetic field, as a function of barrier and well widths and the magnetic field strength. The interaction between light and heavy holes[8] is not considered in our work and we restrict the analysis only to excitons composed by electrons and heavy holes. Within the effective mass approach, we expand the excitonic wave-function, in a orthogonal basis formed by products of electron and hole wave-functions in the growth direction z, and one particle solutions of the magnetic Hamiltonian in the $x-y$ plane.

The Coulomb potential between electrons and holes produces off-diagonal terms by mixing our basis states. We obtained the energies and wave-functions by diagonalizing the excitonic Hamiltonian in a truncated basis.

In contrast to the majority of works in the literature[1,2,4,9], our basis set is orthogonal[5], and we do not use a variational method.

We applied our method to study the first excitonic states, in $GaAs$ ($Al_xGa_{1-x}As$) heterostructures. For comparison purposes in the symmetric case, we used the parameters of Ref. 4. Our analysis of the basis states involved in the excitonic wave-function for different quantum wells geometries, should be helpful in similar studies of $III-V$ and $II-VI$[8,10,11] systems.

II. FORMALISM

The effective mass Hamiltonian for excitons in a double quantum well in the presence of a magnetic field pointing towards z, in the diagonal approximation[12] can be written as

$$H = H_0(z_e) + H_0(z_h) + H_{mag}(\rho) + V_{coul}(\rho, |z_e - z_h|). \tag{1}$$

$H_0(z_e)$ is the 1-dimensional Hamiltonian for electrons,

$$H_0(z_e) = p_{ze}^2/2m_{ze} + V_e(z_e), \tag{2}$$

$H_0(z_h)$ is the 1-dimensional Hamiltonian for holes,

$$H_0(z_h) = p_{zh}^2/2m_{zh} + V_h(z_h), \tag{3}$$

and $V_e(z_e)$ ($V_h(z_h)$) is the potential that defines the double quantum well for electrons (holes) in the five regions of z, shown in Fig. 1. $H_{mag}(\rho)$ is the magnetic Hamiltonian in the symmetric gauge, which depends on the relative coordinates of electrons and holes in the $x-y$ plane,

$$H_{mag} = \frac{(\vec{p} - q\vec{A})^2}{2\mu} + \frac{qB}{m_{h,x-y}} l_z, \tag{4}$$

where $\vec{p}$, μ and $m_{h,x-y}$ are the momentum operator, reduced mass and hole mass, defined in the $x-y$ plane.

$V_{coul}(\rho, |z_e - z_h|)$ is the Coulomb potential between electrons and holes, including an effective dielectric constant for the system.

We expanded the solution of the Hamiltonian 1, as a lineal combination of products of eigenfunctions of the magnetic Hamiltonian in the $x-y$ plane (4), and eigenfunctions of the electron and hole Hamiltonians in the z direction (2 and 3),

$$\Psi_n^{exc} = \sum_{\nu_\rho,\nu_e,\nu_h} C^n_{\nu_\rho,\nu_e,\nu_h} \psi_{\nu_\rho}(\rho,\phi)\psi_{\nu_e}(z_e)\psi_{\nu_h}(z_h), \tag{5}$$

in which

$$\begin{aligned} \psi_{\nu_\rho,l} = {} & \tfrac{1}{2\pi} \left(\tfrac{2(n-l/2-|l|/2) g_B^{|l|+1}}{(|l|/2+n-l/2)!} \right)^{1/2} e^{il\phi} (\tfrac{\rho}{i})^{|l|} \\ & \times \; e^{-g_B\rho^2/2} L^{|l|}_{n-l/2-|l|/2}(g_B\rho^2), \end{aligned} \tag{6}$$

where only $l = 0$ functions are considered, and $g_B = \frac{qB}{2\hbar}$. The electron wave-function defined in the five regions of z, shown in Fig. 1, is given by

$$\psi(z_e) = \begin{cases} a_1 e^{k_1(z_e - z_1)} \\ a_2 cos(k_2(z_e - z_1)) + a_3 sin(k_2(z_e - z_1)) \\ a_4 e^{k_3(z_e - z_2)} + a_5 e^{-k_3(z_e - z_2)} \\ a_6 cos(k_4(z_e - z_3)) + a_7 sin(k_4(z_e - z_3)) \\ a_8 e^{-k_5(z_e - z_4)}, \end{cases} \tag{7}$$

and the hole wave-function is given by similar expressions.

The Coulomb interaction produces off-diagonal terms by mixing our basis states. In order to obtain the system of equations for the coefficients in the expansion (5), we need to evaluate the Coulomb integral

$$\int d\phi d\rho dz_e dz_h \psi^*_{\nu'_\rho} \psi_{\nu'_e} \psi_{\nu'_h} V_{coul}(\rho, |z_e - z_h|) \psi_{\nu_\rho} \psi_{\nu_e} \psi_{\nu_h}. \tag{8}$$

The ϕ integral is trivial, because of l_z conservation. Using the explicit expansion of Laguerre Polynomials (L_n) in $\psi_{\nu'_\rho}$ and ψ_{ν_ρ} (6), the remaining of integral (8) can be written as a sum of terms of the form:

$$\int_{-\infty}^{\infty} dz_e dz_h \psi_{\nu'_e} \psi_{\nu'_h} \psi_{\nu_e} \psi_{\nu_h} \int_0^\infty \rho d\rho \frac{\rho^{2w} e^{-g_B\rho^2}}{\sqrt{\rho^2 + (z_e - z_h)^2}}. \tag{9}$$

By using

$$\frac{1}{\sqrt{\rho^2 + (z_e - z_h)^2}} = \int_0^\infty J_0(\rho\alpha) e^{-|z_e - z_h|\alpha} d\alpha \tag{10}$$

and after solving the ρ integral, it yields

$$\int_0^\infty d\alpha(\frac{\alpha^2}{4g_B})^m e^{\frac{-\alpha^2}{4g_B}} \int_{-\infty}^{\infty} dz_e dz_h \psi_{\nu'_e}\psi_{\nu'_h} e^{-|z_e-z_h|\alpha}\psi_{\nu_e}\psi_{\nu_h}. \qquad (11)$$

The z_e and z_h integrals can be solved analytically. The evaluation of these integrals is cumbersome due to the large number of terms, resulting from the five different regions of the potential. The z_e and z_h integrals contain both, decoupled terms in which the z_e and z_h integrals are independent of each other, and coupled terms where the integration limits of the z_h integral contains z_e. The remaining α integral must be calculated numerically.

Diagonalizing the system of equations resulting for the coefficients in the expansion (5), in a truncated basis, we obtained the energies and wave-functions for the first excitonic levels. Evaluating the oscillator strength

$$f_n = \frac{|\int dz \Psi_n^{exc}(\rho=0, z_e=z, z_h=z)|^2 |\vec{\epsilon}\cdot\vec{p}_{eh}|^2}{m_0 E_n} \qquad (12)$$

we obtained the optical absorption spectra.

III. RESULTS

We calculated the excitonic energy levels and the magneto-optical absorption spectra for symmetric and asymmetric double quantum wells, composed by $GaAs$ wells and $Al_xGa_{1-x}As$ barriers ($x = 0.3$). The band gap used in our calculations is given by $E_g(x) = 1.52 + 1.36x + 0.22x^2$. The band gap offset considered was a sixty percent for the conduction band and a forty percent for the valence band. For comparison purposes in the symmetric case, we used the same simplified masses of Ref. 4, for all five regions in the double quantum well. The electron mass considered was $m_e = 0.067m_0$, the $x-y$ plane heavy hole mass, $m_{hh,x-y} = 0.1m_0$, the $z-axis$ heavy hole mass $m_{hh,z} = 0.45m_0$ and the light hole masses $m_{lh,x-y} = 0.2m_0$, $m_{lh,z} = 0.08m_0$, which corresponds to $\gamma_1 = 7.36$ and $\gamma_2 = 2.57$. We considered a dielectric constant $k_0 = 12.5$.

It was enough to consider in our calculations a truncated basis composed of twelve Landau wave-functions, four electronic wave-functions and four heavy hole wave-functions.

A. Symmetric double quantum well

In this section we present our results for the excitonic energy levels in symmetric double quantum wells as a function of wells and barrier widths, ranging from zero to large values, in a 10 $Tesla$ magnetic field. Also, we present the optical absorption spectra, including broadening for each possible optical transition.

Fig. 2a shows the binding energy of the ground state, for a 25 Å barrier and for both wells widths ranging from 0 to 200 Å . For zero well width, the exciton is tridimensional and it corresponds to bulk $Al_{.3}Ga_{.7}As$. For non-zero well width, the exciton is localized within the wells, reaching a maximum binding energy at a certain well width which corresponds to a maximum two-dimensional character. For further increase in the wells width, the binding energy decreases and the exciton evolves towards a tridimensional $GaAs$ exciton for thick wells. This behavior of the ground state compares very well with the results of Ref. 4, although our energies are 0.5 meV lower.

Fig. 2b shows the ground state binding energy for wells width fixed in 100 Å , and barrier width ranging from 0 to 100 Å . As the barrier width is varied from zero to infinity, we move from the case of a single quantum well (width: $Lw1 + Lw2$), towards two independent quantum wells of width $Lw1$ and $Lw2$. It is known that when the system size decreases, the exciton binding energy increases, accordingly the binding energy starts in a value which corresponds to a single quantum well of width $Lw1 + Lw2$ and ends in a larger value that corresponds to each decoupled quantum well. The binding energy decreases for thinner barriers, because the wave-functions have a large amplitude within the barrier, which is equivalent to a single quantum well wider than $Lw1 + Lw2$. In this case we obtain an excellent agreement with Ref. 4.

Fig. 3a shows the ground state and higher excitonic levels in a symmetric double quantum well, for 100 Å wells and barrier width ranging from 0 to 50 Å . It can be seen that the second energy level (optically prohibited in the symmetric case), gets closer to the ground state for wider barriers. This is a typical behavior, when we go from a situation of coupled quantum wells towards one of two decoupled wells having degenerate energies. In this case the Coulomb potential do not mix states with different symmetry under simultaneous interchange of z_e by $-z_e$ and z_h by $-z_h$. In terms of our base wave-functions, the first two excitonic states evolve from e_1h_1 (first electron - first hole, exciton) and e_1h_2 (first electron - second hole, exciton), towards $e_1h_1 + e_2h_2$ and $e_1h_2 + e_2h_1$ as the barrier get wider. This behavior was noted (without magnetic field) in Ref. 2 and corresponds to the ground state evolving towards $e_Lh_L + e_Rh_R$, in terms of a basis of single quantum well wave-functions, corresponding to the electron (or hole) localized in the left well L or the right well R. This classification in terms of L and R states, will be useful in explaining the optical absorption spectra for thick barriers.

In Fig. 3b, we show the optical absorption spectra for 100 Å wells, with the central barrier ranging from 0 to 30 Å . The state e_2h_2 evolves toward $e_1h_1 - e_2h_2$ getting close to the state $e_1h_1 + e_2h_2$. This state disappear from the spectra, because is evolving towards $e_Rh_L + e_Lh_R$, where the coupling between electron and hole wave-functions decreases, as the electron and the hole are localized in separated wells. The finite energy separation between these states for wide barriers, is a consequence of the small binding energy for the $e_1h_1 - e_2h_2$ state, and corresponds to the binding energy for the $e_1h_1 + e_2h_2$ state for very large barriers. For thin barriers, one small peak between e_1h_1 and e_2h_2 , corresponding to e_1h_3, can not be distinguished. The other peaks correspond to higher levels and the shoulder in e_2h_2, which evolves growing in size, corresponds to a Landau level of e_1h_1.

The states involved in the anti-crossing (produced for a 10 Å barrier) have a very small oscillator strength, compared to the e_2h_2 state. Because of this, the anti-crossing manifest itself only as small distortion, in the evolution from e_2h_2 towards $e_1h_1 - e_2h_2$, which finally disappear from the spectra for thick barriers, as mentioned previously.

Fig. 4a shows the ground and higher excitonic states (with respect to the first band to band transition) for a symmetric double quantum well, with a central barrier of 25 Å and both wells ranging from 0 to 200 Å . The higher levels show an anticrossing region involving the states e_2h_1 (e_2h_2) and a Landau level. The states e_1h_1 and e_1h_2 evolve towards $e_1h_1 + e_2h_2$ y $e_1h_2 + e_2h_1$.

Fig. 4b shows the calculated optical absorption for the previous case. The anticrossing region (for 45 Å wells) manifests as a reinforcement in the spectral lines, caused by the coincidence of the Landau energy and the energy separation between the e_1h_1 and e_2h_2 states. It can be seen as the e_2h_2 state get close to the e_1h_1 state and loose probability for wide wells.

Previous works only included the coupling between levels, necessary for having the right energy behavior for the excitonic wave-function for thick barriers, and the general belief was that coupling between others levels is of no importance. In our calculation is clear that although this is true for almost all wells and barrier widths, there are regions where another off-diagonal terms must be included, for explaining the anti-crossings that we obtained between higher levels (see Fig. 3a).

B. Asymmetric double quantum well

When going from the symmetric case towards the asymmetric one, states prohibited by the quantum well symmetry can appear in the optical absorption spectra. These states have a small oscillator strength, near the symmetric case, which increases when the z potential is going far from symmetry.

In asymmetric double quantum wells, the excitonic ground state wave-function is mostly localized in the wider well. For $Lw1$ smaller than $Lw2$ the ground state binding energy corresponds to an exciton localized in the right well. As $Lw1$ get closer to $Lw2$, the exciton begin to be present in the left well and the binding energy decreases. When the two wells are of the same width, the exciton is localized in both wells (symmetric case) and the binding energy reach a local minima. For $Lw1$ bigger than $Lw2$, the exciton exciton is localized in the left well and the binding energy increases. After this, the binding energy reach a maxima and decreases towards the tridimensional limit of a very thick left well.

Fig. 5a shows the ground and higher excitonic states, for a 100 Å right well, a 35 Å barrier and a 10 $Tesla$ magnetic field, for the left well ranging from 60 Å to 100 Å . The ground state remains fixed in energy and corresponds to an exciton localized in the right well (the ground state binding energy behavior, explained previously, can not be observed in the scale of Fig. 5). The second excitonic state, prohibited and degenerate in energy with the ground state (for thick barriers) in the symmetric case, separates from the ground state when the left well width decreases. For a 85 Å left well, this state interacts with the third state, producing an anti-crossing. In the anticrossing region, these states lose their identity, transforming into $e_1h_2 + e_2h_2$ and $e_1h_2 - e_2h_2$. From analyzing the energies and wave-functions in our basis states, we see that this anti-crossing is not originated by a crossing between electron (or hole) levels of the right and left wells (see Ref. 3), as for almost all left well widths of Fig. 5a, the electron (hole) levels e_1, e_3 (h_1, h_3) are already localized in the right well and e_2, e_4 (h_2, h_4) in the left well. These anti-crossings, are a consequence of the strong interaction between excitonic states, when the levels corresponding to the direct exciton e_2h_2 (e_Lh_L) and indirect exciton e_1h_2 (e_Rh_L), get close in energy. The different behavior in these energy levels, when one of the wells width is varied, is originated by the different spatial character of excitons localized in only one well (direct) and excitons where electron and hole are localized in different wells (indirect). As can be seen from Fig. 5b, both excitonic states have a large oscillator strength in the anti-crossing region, and because the energy separation is approximately 4 meV between them, this anti-crossing could be observed experimentally.

In Fig. 6a we show the excitonic states for a 85 Å left well and a 100 Å right well in a 10 $Tesla$ magnetic field, as a function of the barrier width. It is clear the way the anti-crossing states evolve and get separated in energy as the barrier is decreased. When these energy levels go far from each other, the probability of being created optically decreases. This would make difficult to obtain experimentally this anti-crossing, for barriers smaller than 35 Å . For wider barriers, the direct exciton e_2h_2 has a lower energy than the indirect exciton e_1h_2, as a consequence of the large binding energy of e_2h_2, relative to e_1h_2. These different binding energies are a consequence of the large spatial separation of the wave-functions corresponding to e_1 and h_2.

These anti-crossings has not be obtained previously. We think that it is important to carry out an experimental study, of the correlation in the optical absorption spectrum, for the energies of the second and third excitonic states, in the anti-crossing region. Also could be interesting, to study the possible relationship of the states $e_1h_2 + e_2h_2$ and $e_1h_2 - e_2h_2$ with charged excitons[13–15], because these states involve one particle wave-functions, corresponding to two electrons and one hole states.

C. Magnetic field effects

Increasing the magnetic field in a symmetric or asymmetric double quantum well, produces a shift in the excitonic energy levels towards higher energies and an increase in the binding energy. The increase in the binding energy is a consequence of two effects: First, the wave-function confinement in the $x - y$ plane produces a stronger interaction in the $z - axis$, as the electron and hole wave-functions penetrates more in the barrier. Second, the binding between electron and hole in the plane increases, because their wave-functions are confined to a smaller region.

The large binding between electron and hole obtained when increasing the applied magnetic field, is similar to a change in the barrier and well width. This can be used to study these systems in regions of interest, without the need for the growth of many different samples.

In Fig. 6b, we show the magnetic field effects for the asymmetric double quantum well, in the anti-crossing region of Fig. 6a. When the magnetic field ranges from 0 to 40 $Tesla$, the energy levels are shifted towards a bigger energy and the binding is stronger. The behavior for the indirect excitonic levels is similar to decreasing the barrier width in the anti-crossing region. The direct exciton binding energy also increases, as a consequence of the wave-function localization in the $x - y$ plane. Because the direct exciton has a larger binding energy than the indirect exciton for large magnetic fields, this level goes below the indirect exciton level for strong magnetic fields.

IV. CONCLUSION

In this work we studied the energies and oscillator strength, for several excitonic **S** levels in a double quantum well, in a magnetic field pointing in the growth direction z. We calculated the excitonic binding energy and optical absorption for type I symmetric and asymmetric double quantum wells, as a function of barrier and well (or wells) widths.

In our method we used an orthogonal basis and we do not employed a variational method. Specific calculations for the ground state excitonic binding energy, in symmetric double quantum wells, are in excellent agreement with the work of Cen-Bajaj[4]. In contrast to the Dignam-Sipe[2] work, we used basis functions of single particle solutions of the double quantum well, and our method is valid for all barrier width.

To our understanding, this is the first theoretical calculation, in a symmetric and asymmetric double quantum well, that is valid for all barrier widths. This allow us to study these systems, from the case of a single quantum well (null barrier) to the case where both wells get decoupled.

We do not know another theoretical calculation that predict the anti-crossings between excitonic levels, that we obtain as a consequence of including in our method all the coupling between our basis wave-functions.

ACKNOWLEDGMENTS

We want to acknowledge the hospitality of the people in the electronic department in Glasgow University, specially to C. Sotomayor, D. Hutchings and J. Arnold. We also want to acknowledge a Conicyt-British Council grant for a research student-ship given to Francisco Vera, and to G. Fuster for many discussions on this topic. This work was supported by the Fondecyt projects 1950190,1970119 and a Conicyt doctoral fellowship.

---

[1] T. Kamizato and M. Matsuura, Phys. Rev. B **40**,8378 (1989).
[2] M. Dignam and J. Sipe, Phys. Rev. B **43**,4084 (1991).
[3] R. Ferreira,C. Delalande,H. W. Liu,G. Bastard, B. Etienne and J. F. Palmier, Phys. Rev. B **42**,9170 (1990).
[4] J.Cen and K. Bajaj, Phys. Rev. B **46**,15280 (1992).
[5] A. Dzyubenko and A. Yablonskii, Phys. Rev. B **53**,16355 (1996).
[6] M. Bayer,V. B. Timofeev,F. Faller,T. Gutbrod and A. Forchel, Phys. Rev. B **54**,8799 (1996).
[7] R. Ferreira and G. Bastard, Rep. Prog. Phys. **60**,345 (1997).
[8] A. Hernandez and A. Ramos, J. Appl. Phys. **80**,1547 (1996).
[9] I. Linnerud and K. Chao, Phys. Rev. B **49**,8487 (1994).
[10] S. Ten,M. F. Krol,P. T. Guerreiro and N. Peyghambarian, Appl. Phys. Lett. **69**,3387 (1996).
[11] H. Haas,N. Magnea and L. Dang, Phys. Rev. B **55**,1563 (1997).
[12] G. Bastard, wave mechanics applied to semiconductor heterostructures, les editions de physique (1990), p. 139.
[13] A. J. Shields,J. L. Osborne,D. M. Whittaker, M. Y. Simmons,M. Pepper and D. A. Ritchie, Phys. Rev. B **55**,1318 (1997).
[14] G. Finkelstein,H. Shtrikman and I. Barjoseph, Surface Science **362**,357 (1996).
[15] P. Lelong and G. Bastard, Solid State Commun. **98**,819 (1996).

FIG. 1. Potential profile in the z direction for electrons and holes.

FIG. 2. Exciton binding energy for a symmetric double quantum well ($B = 10\ Tesla$). (a) Plotting as a function of the width of the wells, for a barrier of 2.5 nm. (b) As a function of the width of the barrier, for wells of 10 nm.

FIG. 3. Exciton energy levels for a symmetric double quantum well as a function of the barrier width, for wells of 10 nm ($B = 10\ Tesla$). (a) Evolution of the excitonic states, showing the most important base states present in the exciton wave-function (ij means $e_i h_j$). (b) Calculated optical absorption for these states, each curve represent a different barrier width showed by the y axis, the peaks show the optical absorption refered to the bottom of each curve.

FIG. 4. Exciton energy levels for a symmetric double quantum well as a function of the wells width, for a barrier of 2.5 nm ($B = 10\ Tesla$). (a) Evolution of the excitonic states. For clarity in representing these states, we subtracted the first energy level in this system when the Coulomb potential is not taken into account. (b) Calculated optical absorption for these states.

FIG. 5. Exciton energy levels for an asymmetric double quantum well as a function of the left well width, for a barrier of 3.5 nm and a right well width of 10 nm ($B = 10\ Tesla$). (a) Evolution of the excitonic states. (b) Calculated optical absorption for these states.

FIG. 6. Exciton energy levels for an asymmetric double quantum well, with a left well width of 8.5 nm and right well width of 10 nm. (a) As a function of the barrier width ($B = 10\ Tesla$). (b) As a function of the magnetic field for a barrier of 3.5 nm. (numbers enclosed in parenthesis indicates a small contribution of this states, to the exciton wave-function)

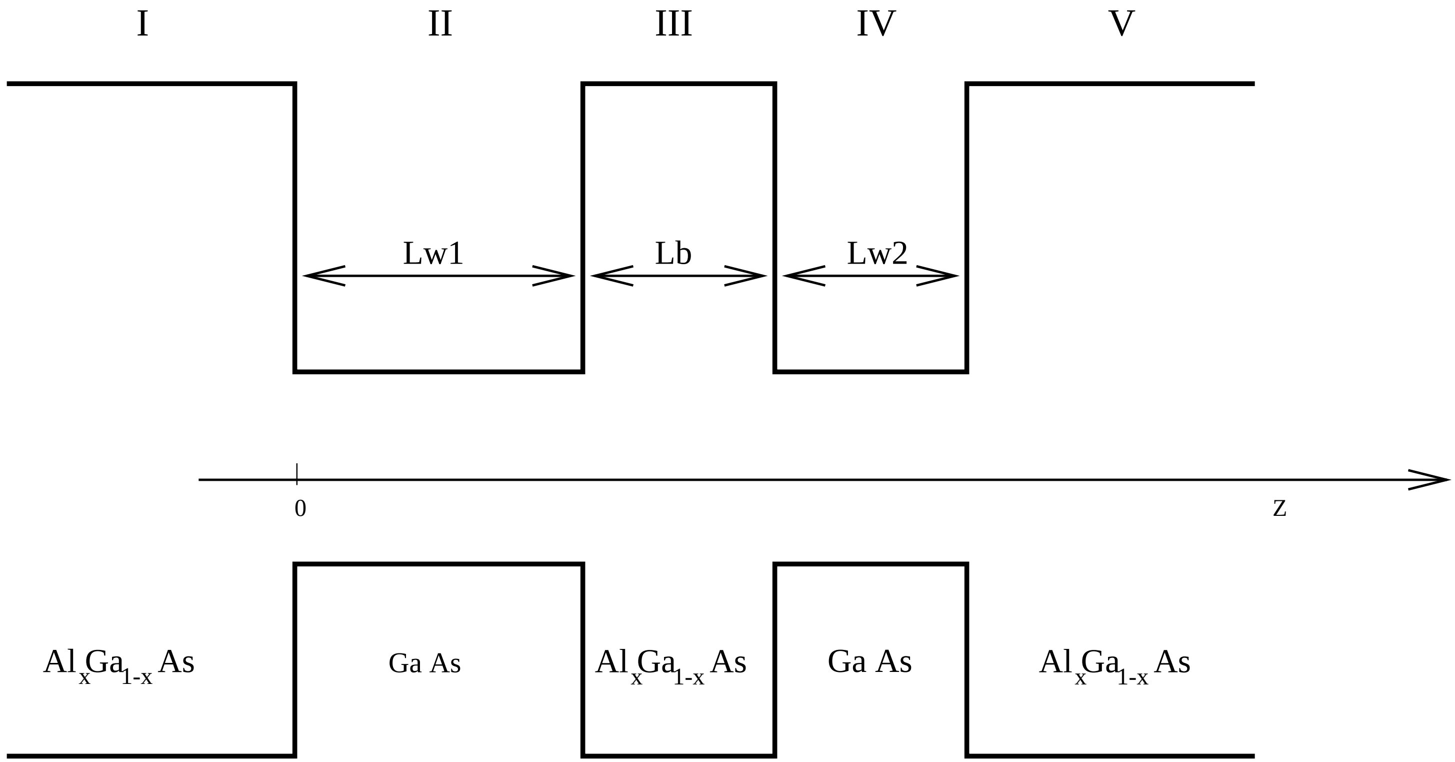
I
II
III
IV
V
Lw1
Lb
Lw2
0
z
$Al_xGa_{1-x}As$
Ga As
$Al_xGa_{1-x}As$
Ga As
$Al_xGa_{1-x}As$

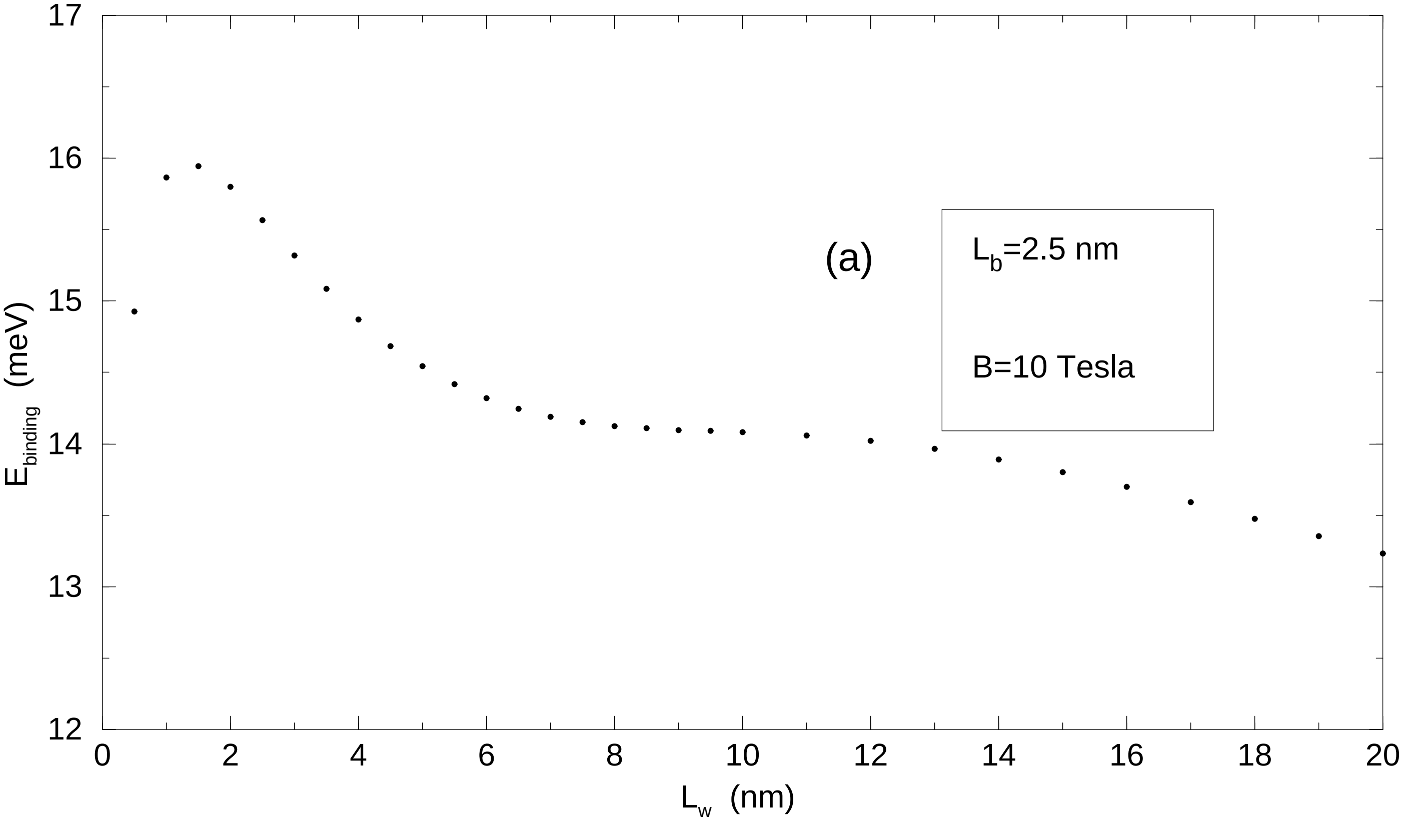
(a)
L_b=2.5 nm
B=10 Tesla
$E_{binding}$ (meV)
L_w (nm)
12
13
14
15
16
17
0
2
4
6
8
10
12
14
16
18
20

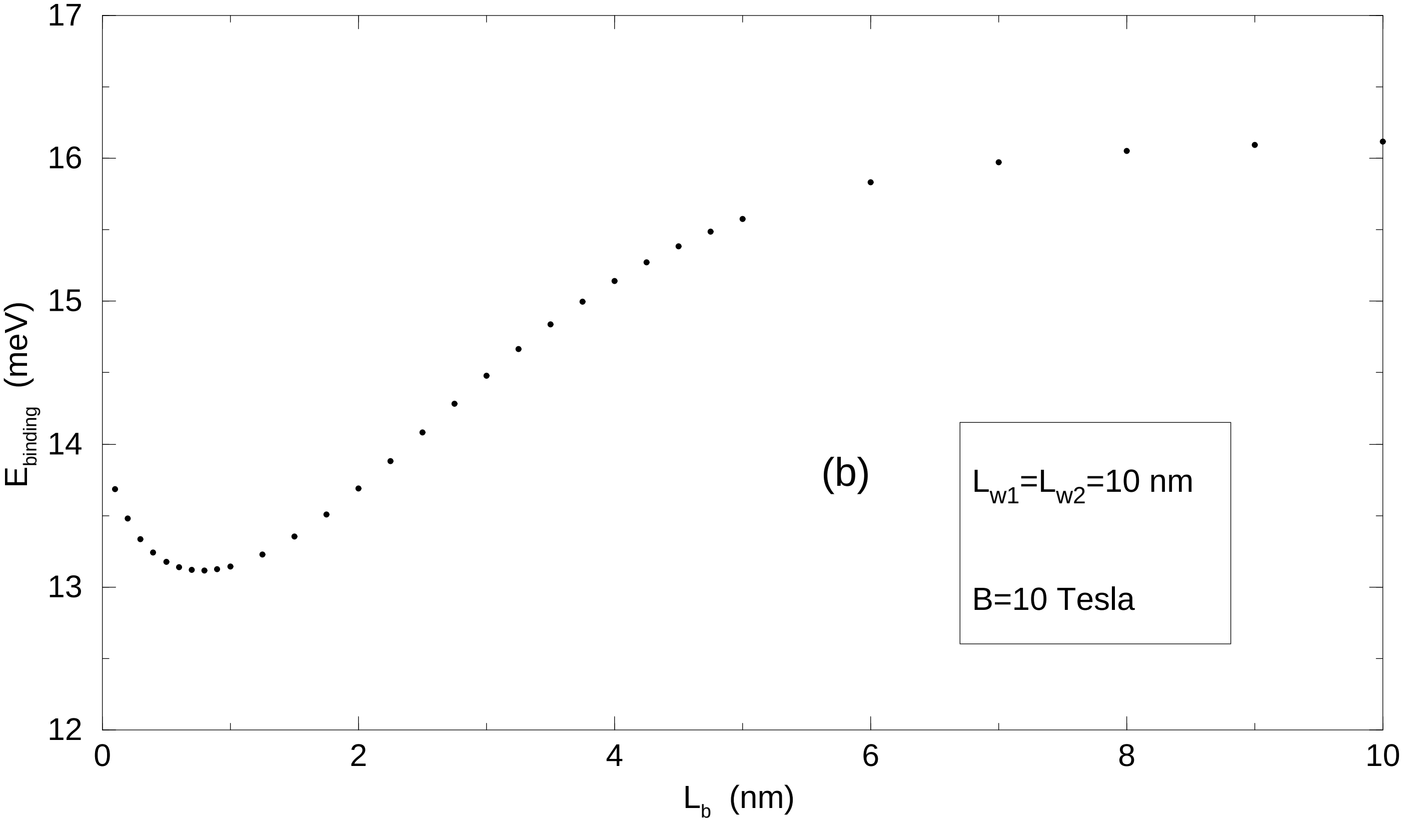
(b)
L_{w1}=L_{w2}=10 nm
B=10 Tesla
$E_{binding}$ (meV)
L_b (nm)
12
13
14
15
16
17
0
2
4
6
8
10

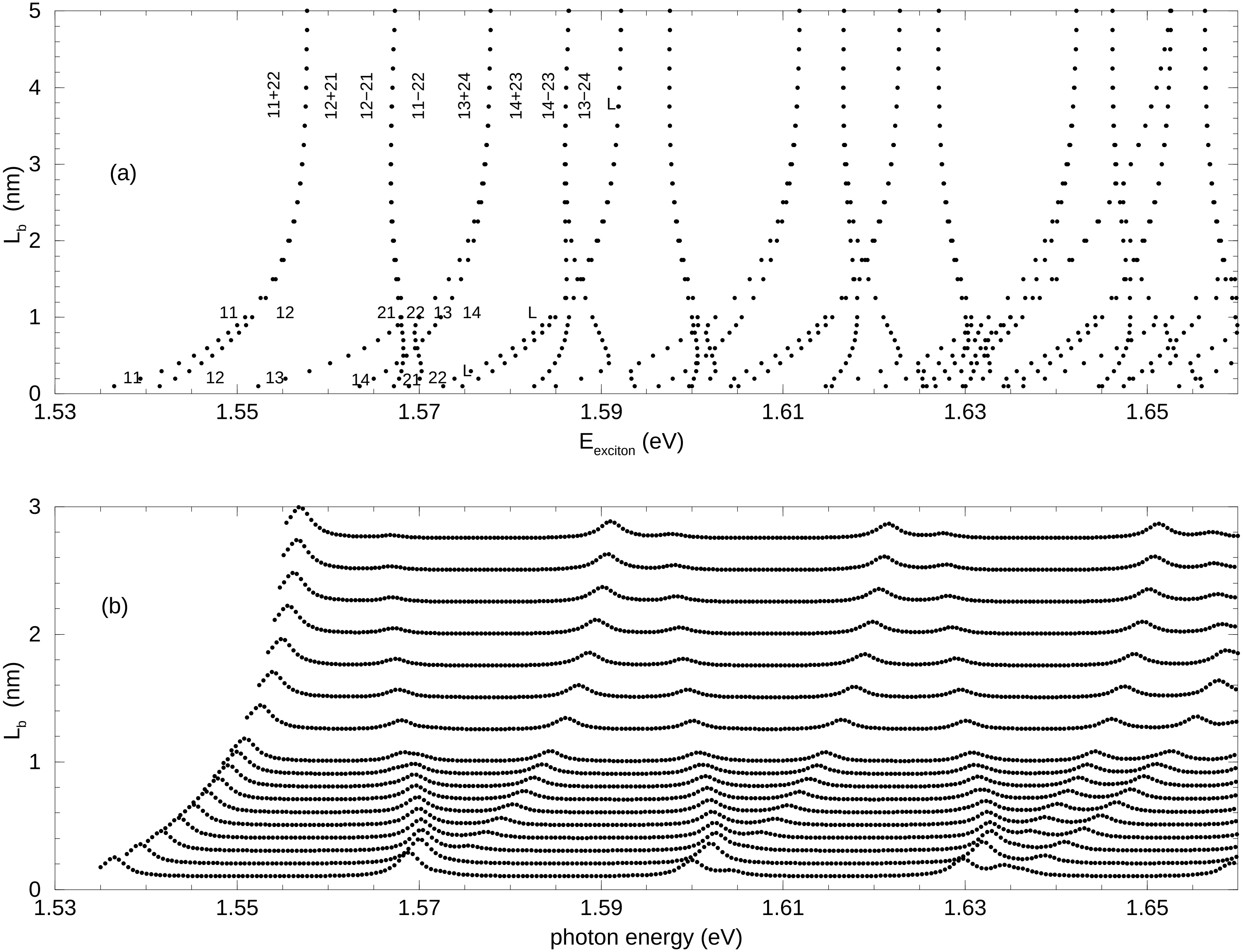

(a)
5
4
3
2
1
0
L_b (nm)
11+22
12+21
12−21
11−22
13+24
14+23
14−23
13−24
L
11
12
21
22
13
14
L
11
12
13
14
21
22
L
1.53
1.55
1.57
1.59
1.61
1.63
1.65
E_exciton (eV)
(b)
3
2
1
0
L_b (nm)
1.53
1.55
1.57
1.59
1.61
1.63
1.65
photon energy (eV)

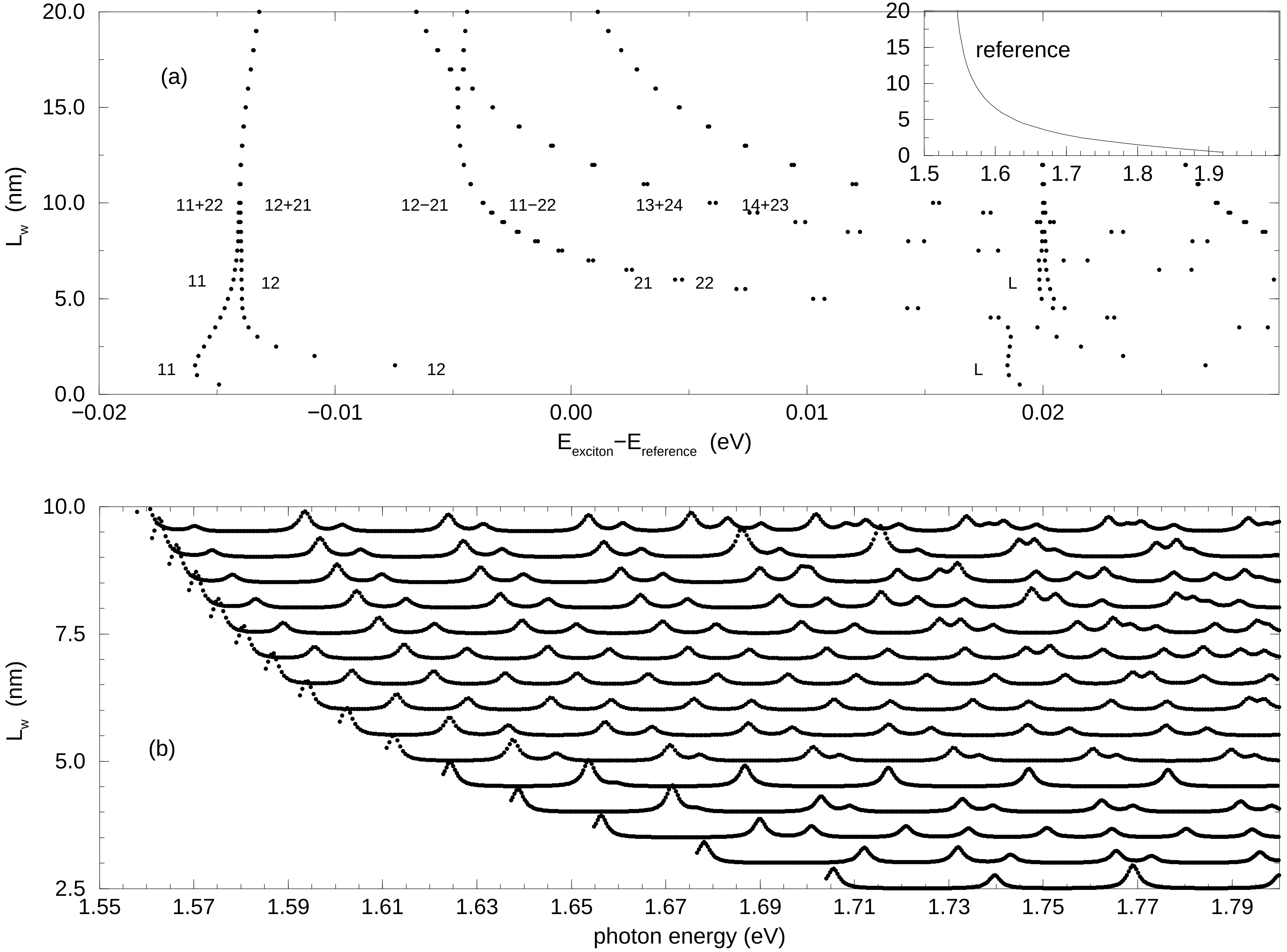
(a)
20.0
15.0
10.0
5.0
0.0
L_w (nm)
11+22
12+21
12−21
11−22
13+24
14+23
11
12
21
22
L
11
12
L
−0.02
−0.01
0.00
0.01
0.02
E_exciton−E_reference (eV)
reference
20
15
10
5
0
1.5
1.6
1.7
1.8
1.9
(b)
10.0
7.5
5.0
2.5
L_w (nm)
1.55
1.57
1.59
1.61
1.63
1.65
1.67
1.69
1.71
1.73
1.75
1.77
1.79
photon energy (eV)

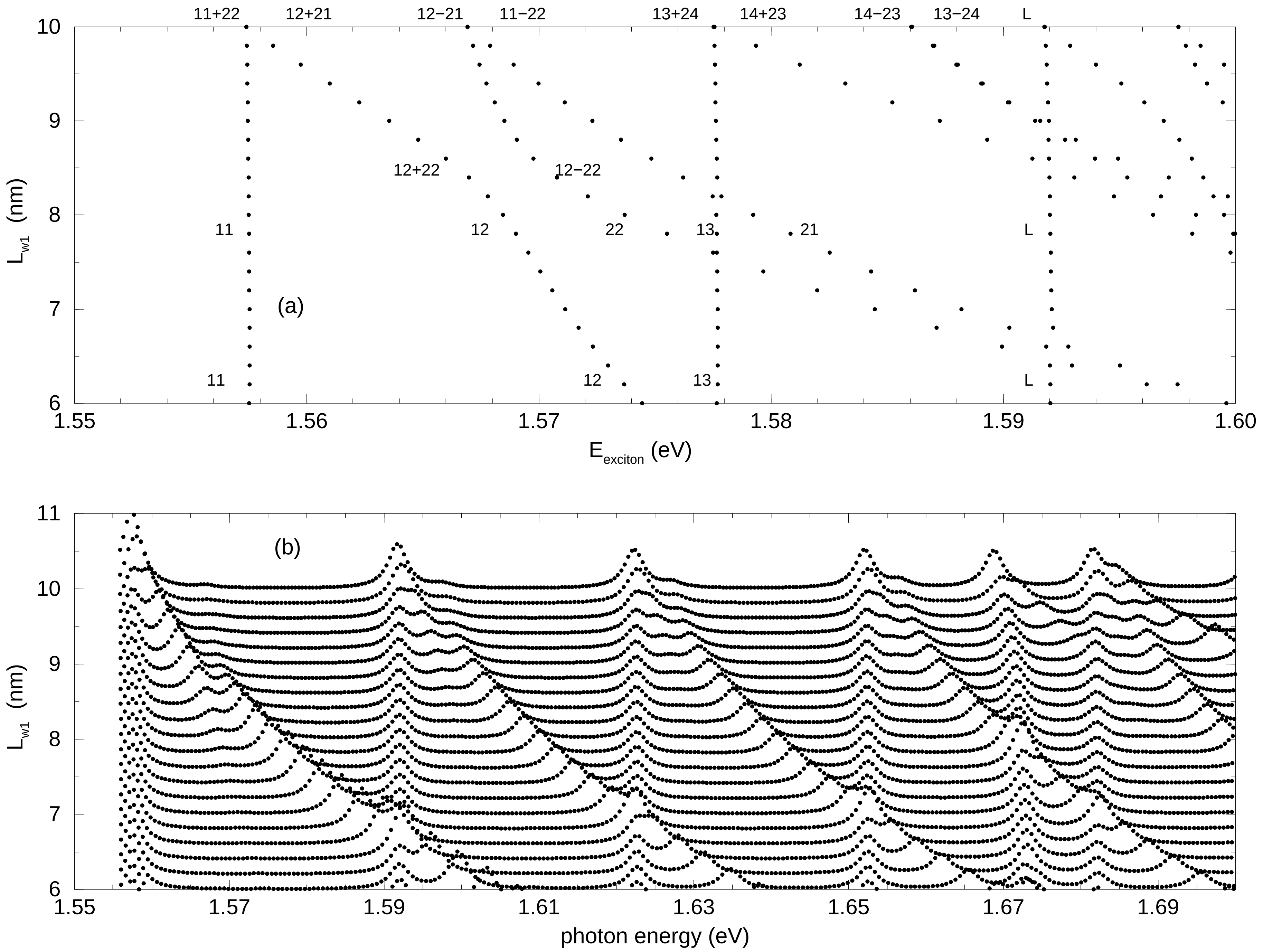
11+22
12+21
12−21
11−22
13+24
14+23
14−23
13−24
L
12+22
12−22
11
12
22
13
21
L
11
12
13
L
(a)
L_{w1} (nm)
10
9
8
7
6
1.55
1.56
1.57
1.58
1.59
1.60
$E_{exciton}$ (eV)
(b)
L_{w1} (nm)
11
10
9
8
7
6
1.55
1.57
1.59
1.61
1.63
1.65
1.67
1.69
photon energy (eV)

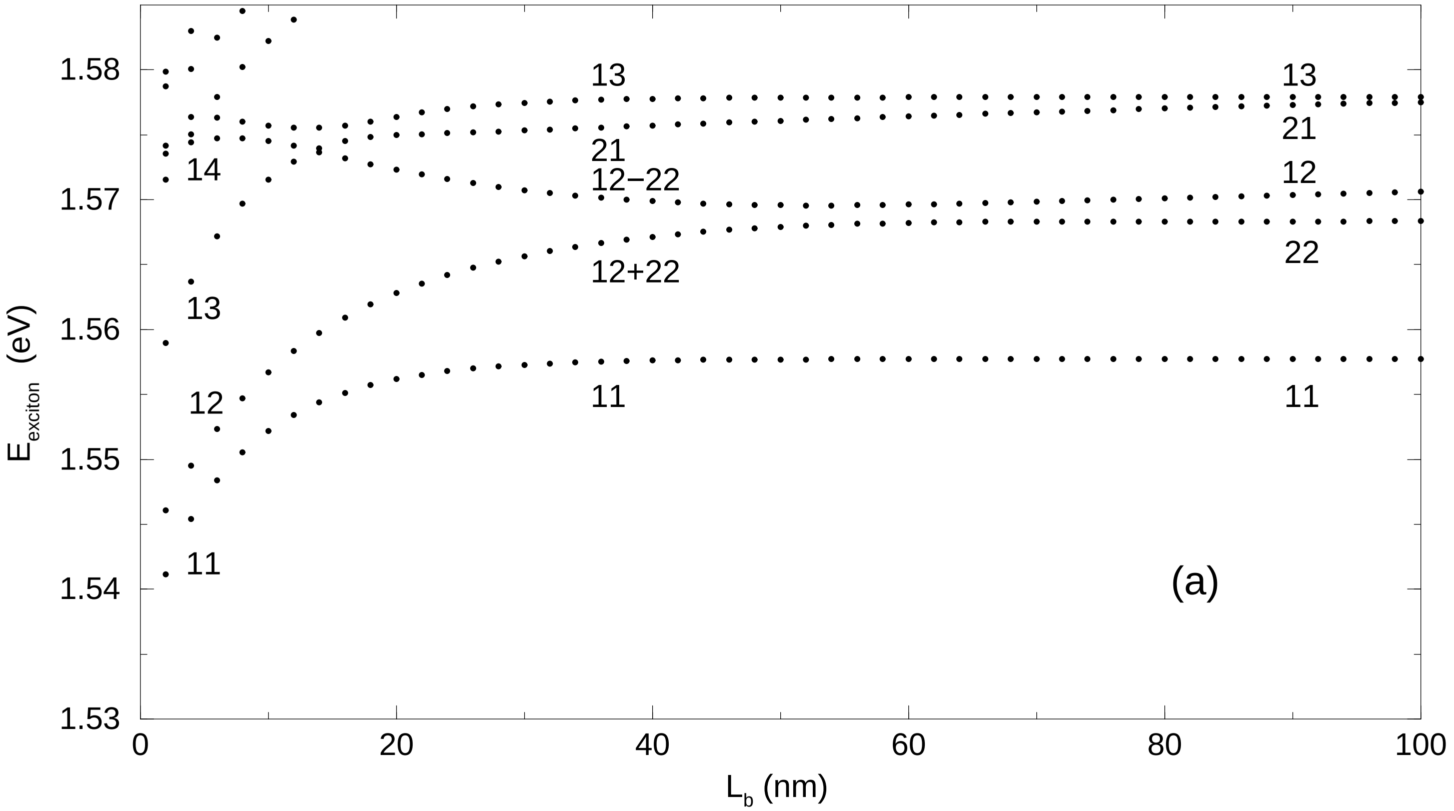
1.58
1.57
1.56
1.55
1.54
1.53
$E_{exciton}$ (eV)
0
20
40
60
80
100
L_b (nm)
13
21
12−22
12+22
11
14
13
12
11
13
21
12
22
11
(a)

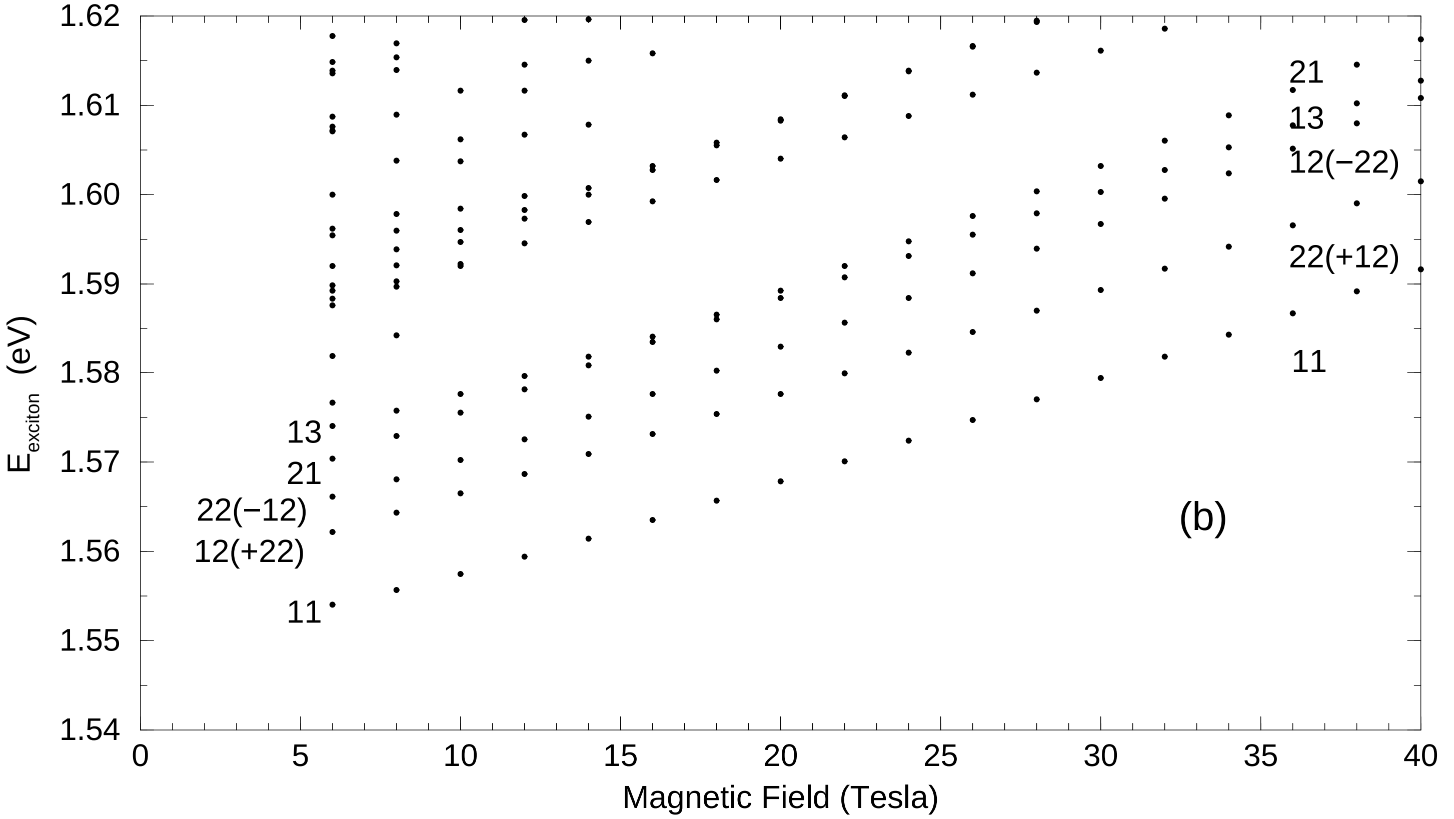
1.62
1.61
1.60
1.59
1.58
1.57
1.56
1.55
1.54
$E_{exciton}$ (eV)
0
5
10
15
20
25
30
35
40
Magnetic Field (Tesla)
13
21
22(−12)
12(+22)
11
21
13
12(−22)
22(+12)
11
(b)